Dark matter imprint on ^{8}B neutrino spectrum

Ilídio Lopes, Joseph Silk

Dark matter imprint on ^{8}B neutrino spectrum

Ilídio Lopes[1,*] and Joseph Silk[2,3,4,†]

[1]*Centro de Astrofísica e Gravitação—CENTRA, Departamento de Física, Instituto Superior Técnico—IST, Universidade de Lisboa—UL, Av. Rovisco Pais 1, 1049-001 Lisboa, Portugal*

[2]*Institut d'Astrophysique de Paris, UMR 7095 CNRS, Université Pierre et Marie Curie, 98 bis Boulevard Arago, Paris 75014, France*

[3]*Beecroft Institute of Particle Astrophysics and Cosmology, 1 Keble Road, University of Oxford, Oxford OX1 3RH, United Kingdom*

[4]*Department of Physics and Astronomy, 3701 San Martin Drive, The Johns Hopkins University, Baltimore, Maryland 21218, USA*

(Received 5 May 2018; published 11 January 2019)

The next generation of solar neutrino detectors will provide a precision measure of the ^{8}B electron-neutrino spectrum in the energy range from 1–15 MeV. Although the neutrino spectrum emitted by ^{8}B β-decay reactions in the Sun's core is identical to the neutrino spectrum measured in the laboratory, due to vacuum and matter flavor oscillations, this spectrum will be very different from that measured on Earth by the different solar neutrino experiments. We study how the presence of dark matter (DM) in the Sun's core changes the shape of the ^{8}B electron-neutrino spectrum. These modifications are caused by local variations of the electronic density and the ^{8}B neutrino source, induced by local changes of the temperature, density and chemical composition. Particularly relevant are the shape changes at low and medium energy range ($E_\nu \leq 10$ MeV), for which the experimental noise level is expected to be quite small. If such a distortion in the ^{8}Bν_e spectrum were to be observed, this would strongly hint in favor of the existence of DM in the Sun's core. The ^{8}B electron-neutrino spectrum provides a complementary method to helioseismology and total neutrino fluxes for constraining the DM properties. In particular, we study the impact of light asymmetric DM on solar neutrino spectra. Accurate neutrino spectra measurements could help to determine whether light asymmetric DM exists in the Sun's core, since it has been recently advocated that this type of DM might resolve the solar abundance problem.

DOI: 10.1103/PhysRevD.99.023008

I. INTRODUCTION

Solar neutrino detectors have been one of the beacons of particle physics, both by leading the way in discovering the basic properties of particles, including the nature of neutrino flavor oscillations, and by being responsible for developing pioneering techniques in experimental neutrino detection [e.g., [1–3]]. The next generation of detectors like the DUNE Experiment [4], the CJPL Laboratory [5], the JUNO Observatory [6], and the LENA detector [3], will measure with high precision the neutrino fluxes and neutrino spectra of a few key solar nuclear reactions, such as the electron-neutrino (^{8}Bν_e) spectrum produced by the β-decay of ^{8}B [7,8]. This will allow us to probe in detail the Sun's core, including the search for unknown physics processes. Moreover, the high quality of the data will enable the development of inversion techniques for determining basic properties of the solar plasma [e.g., [9]]. Specific examples can be found in Balantekin *et al.* [10], Davis [11] and Lopes [12]. Equally, solar neutrino data can be used to find specific features associated with new physical processes [e.g., [13,14]], such as the possibility of an isothermal solar core associated with the presence of DM [15].

The ^{8}Bν_e spectrum emitted by the nuclear reactions in the Sun's core is identical to that determined by current laboratory experiments [e.g., [16–20]]. Bahcall [21] has shown that the corrections on the shape of neutrino energy spectra caused by the surrounding plasma in the Sun's core are negligible. For example, the corrections related with the thermal motions of the colliding ions are negligible, as the thermal velocity of ions is much smaller than the velocity of light. Given that the ^{8}Bν_e spectrum shape is well-known and we know that the solar plasma does not influence

*ilidio.lopes@tecnico.ulisboa.pt
†silk@astro.ox.ac.uk

significantly the nuclear reactions occurring in the Sun's core, the changes detected in the $^8B\nu_e$ spectrum will be mostly due to neutrino flavor oscillations induced by matter [a process also known as the Mikheyev-Smirnov-Wolfenstein: MSW effect, [22–24]]. These modifications will change not only the overall neutrino flux but, more significantly, modify the neutrino spectrum by affecting in a differential manner the survival probability of electron-neutrinos—depending upon the energy of the emitted neutrino.

The impact of neutrino flavor oscillations on the total neutrino fluxes is extensively documented in the literature [see [2], and references therein], but the impact on solar neutrino spectra has been discussed only briefly. The reason is that neutrino flavor oscillations are expected to be unimportant, because the temperature of the Sun's core is strongly constrained by the total neutrino fluxes. Nevertheless, as we discuss in this article, this is not necessarily the case, mostly because neutrino flavor oscillations due to the MSW effect in the Sun's core depend strongly of the local properties of the solar plasma. Unlike total neutrino fluxes, these give differential information about the physics of the Sun's core. In particular, if light DM is present in the solar core, the amount of electron-neutrinos converted to other flavors will be different from the value found in the standard solar model [SSM, e.g., [25,26]], and consequently their total neutrino fluxes and neutrino spectra will also be different from the SSM. In recent years, significant improvements in the measurement accuracy of solar neutrino fluxes have been instrumental in allowing the use of the Sun to set constraints on the properties of dark matter, including the neutralino [e.g., [27,28]]. and impose limits to the expected neutrino fluxes coming from the Sun due to DM annihilation [e.g., [29]]. Moreover, a large number of different types of asymmetric DM have been discussed in the literature [30–34]. The presence of dark matter in the Sun's core could help solve the long-running solar composition problem [35], a discrepancy between the solar structure inferred from helioseismology and the one computed from a SSM by inputting the most up-to-date photospheric abundances [36,37]. This type of diagnostic has also been successfully extended to other stars, including other sun-like stars [e.g., [38,39]] and neutron stars [40–43]. In addition, such types of studies have also been extended to the first generation of stars [44–48].

In this paper, we show that by measuring the $^8B\nu_e$ solar spectrum, it is possible to constrain the DM content in the Sun's core. This diagnostic complements the total neutrino flux analysis. This is a robust result, as the shape variation of the $^8B\nu_e$ spectrum is uniquely related to the radial variation of the plasma properties in the Sun's core, where the maximum accumulation of DM is expected to occur. This type of diagnostic is particularly useful for testing new types of DM models [e.g., [49,50]], which have a more pronounced impact in the core of the Sun.

II. CURRENT STATUS OF DARK MATTER RESEARCH

In the last few years, several types of light DM particles have been suggested as an ideal DM candidate for a elementary DM particle, motivated by fundamental theoretical arguments in cosmology and particle physics, and by a few positive hints from some direct DM search experiments. Nevertheless, these results are controversial since other experimental detectors have excluded the same DM parameter space.

In favor of the theoretical argument, several DM models succeed in explaining the observed DM relic density [51,52], as a new type of light DM, usually referred to as asymmetric DM [43,53,54]. Unlike symmetric DM, this new type of DM is believed to be produced in the primordial universe by physical mechanisms identical to the production of baryons, known as darkogenesis [e.g., [55–58]], and likewise composed of an unbalanced mixture of particles and antiparticles. The proportionality of DM particles relatively to DM antiparticles is measured by the asymmetry parameter $\eta_{\rm DM}$, which is identical to $\eta_{\rm B}$ for baryons. In the case that the DM is symmetric, i.e., the DM particle is its own antiparticle, $\eta_{\rm DM} = 0$.

The production of asymmetric DM in the early universe is computed by a similar procedure to baryogenesis [e.g., [59,60]]. The origin of such a DM asymmetry is not known; however, as suggested by some extensions to the standard model of particle physics, this could be related to the existence of electric and magnetic dipole moments of some standard particles and possibly new particles [e.g., [61]]. For reference, the current upper limit on the electric dipole moment of the electron is set to 8.7×10^{-29} e cm [62]. Similarly Lopes *et al.* [49] suggest that the magnetic dipole moment of light DM particle could not be larger than 1.6×10^{-17} e cm.

On the experimental side, the findings of DM searches are a puzzle that is difficult to resolve [63]: several experimental collaborations in direct DM searches have found experimental hints that could be related with dark matter detection: DAMA/LIBRA [64,65] and possibly CoGeNT [66,67] observed an annual modulation, CRESST [68] and CDMSSi [69,70] show hints of an excess of events. These experiments seem to indicate the existence of a DM candidate with a mass of ~10 GeV and a scattering cross section on hydrogen and other chemical elements varying between 10^{-41} and 10^{-36} cm^2. The specific value of the scattering cross section is strongly dependent on the DM model used to interpret the data [e.g., [67,71]]. Presently, the null results constraints are from CDMSGe [72], XENON [73,74] and LUX [75]. These experiments found no evidence for an interaction of DM with baryons for the cited mass and scattering cross section range, at least in the case of a contact type of the DM-nucleus interaction models. Nonetheless, there are new theoretical proposals that resolve the differences between

the different experimental results, the most successfully being the long-range DM-nucleus interactions. In these type of DM models, the interaction between DM and baryons is not contactlike, but occurs through a light particle mediator [e.g., [76–79]]. The impact of such a DM particle in the Sun's interior can modify significantly its core structure [36].

III. DARK MATTER AND THE SUN

As is usually done in these studies, we consider that the Sun's evolution in a DM halo is identical to the SSM. Likewise, these solar models are required to reproduce the current Sun observables such as radius and luminosity. Therefore, the models to compute the impact of DM in the evolution of the Sun were obtained as follows: for each set of DM parameters, we compute a solar-calibrated model following the same procedure used to compute a SSM [80], i.e., by automatically adjusting the helium abundance and the convection mixing length parameter until the total luminosity and the solar radius are within 10^{-5} of the present solar values. Typically, a calibrated DM solar model is obtained after a sequence of 10 to 20 intermediate models.

As the accretion of DM by the star produces minor differences in the Sun's core structure and almost no effect in the stellar envelope, these solar models follow the same path as the SSM in the Hertzsprung-Russell diagram. For the solar model of reference, we choose a SSM with a low-metallicity composition [81], usually referred to as low-Z metallicity SSM. This SSM was computed using an updated version of the stellar evolution code CESAM [82]. The code has up-to-date microscopic physics, and in particular uses the nuclear reaction rates from the NACRE Compilation [83]. This SSM predicts solar neutrino fluxes and helioseismic data that are consistent with other SSM models found in the literature [e.g., [26,84]]. In relation to the properties of our standard solar model, this can be found in Lopes and Silk [85].

In a DM halo, a star captures DM from the beginning of the premain sequence until the present age (4.6 Gyr). The efficiency of the star in accumulating DM in its core is regulated by three leading processes: capture, annihilation and evaporation of DM particles.

The total number of particles $N_\chi(t)$ that accumulates inside the Sun at a certain epoch is computed by solving the following differential equation

$$\frac{dN_\chi(t)}{dt} = \Gamma_c - \Gamma_a N_\chi(t)^2 - \Gamma_e N_\chi(t), \tag{1}$$

where Γ_c, Γ_a and Γ_e are the capture, annihilation and evaporation rates. A detailed account about these quantities can be found in Jungman *et al.* [86] and Bertone *et al.* [87]:

Γ_c determines the amount of DM particles captured by the star. This quantity, among others, depends on the radius and escape velocity at each step of the star's evolution. Nevertheless, it is the scattering of the DM particles with baryons which is the leading process in the capture rate. The scattering cross section depends on the mass and spin of the baryon nuclei. As usual, the scattering cross sections of DM particles with nuclei σ_χ can be either a spin-dependent or spin-independent cross section, that are represented by $\sigma_{\chi,SD}$ and $\sigma_{\chi,SI}$. For all of the chemical elements excluding hydrogen, the interaction with a DM particle is of spin-independent type (coherent scattering), for which the scattering cross section scales as the fourth power of the baryon nucleus mass number [e.g., [87]]. For hydrogen, the spin-dependent interaction (incoherent scattering) is also taken into account. In our code the Γ_c expression is computed following the original expression of Gould [88], Gondolo *et al.* [89] as described in Lopes *et al.* [90].

Γ_a depends on the annihilation cross section $\langle\sigma v\rangle_\chi$ of particles and antiparticles. In the current sets of DM models, we are uniquely concerned with $\langle\sigma v\rangle_\chi \approx 0$ as discussed in the previous section. A detailed account about the differences between the s-wave and p-wave DM annihilation channels can be found in Lopes and Silk [33].

Γ_e determines the amount of particles that evaporates from the Sun. In our study we use an approximate expression computed for sun-like stars by Busoni *et al.* [91] from the original work of Griest and Seckel [92]. Nevertheless, this should not much affect our result as we restrict our analysis to DM particles with a mass above 4 GeV, for which evaporation is not significant [93].

In this study, the focus is on the interaction of DM with chemical elements heavier than hydrogen. The impact related to the capture of DM by the scattering off hydrogen was previously studied by Frandsen and Sarkar [31], among others.

Our DM models, if not stated otherwise, have the following properties: the DM particles in the halo follow a Maxwell-Boltzmann velocity distribution, with a thermal velocity $v_{\rm th} = 270$ km/s; the density of the DM halo is equal to 0.38 GeV cm^{-3} [e.g., [94]]; and the stellar velocity of the Sun is $v_\star = 220$ km/s. The mass of the DM particle m_χ, and the spin-independent and dependent scattering cross sections with baryons $\sigma_{\chi,SD}$ and $\sigma_{\chi,SI}$ were chosen to be in agreement with the current experimental bounds for light DM particles. In particular, the spin-dependent and scattering cross section $\sigma_{\chi,SD}$ is equal to 10^{-46} cm^2. It is worth noting that, unlike in previous studies, we solve numerically equation (1), the equation that regulates the accumulation of DM inside the star [49].

The DM impact on the star at each stage of evolution is determined mostly by $N_\chi(t)$, the number of DM particles accumulated by the star. Once the DM particles are captured by the Sun, these drift towards the Sun's central region, providing the star with a new energy transport mechanism, which then removes energy from the core

towards the more external layers of the star. The efficiency of this transport of energy depends mainly on the ratio between the mean free path of the DM particles through the solar plasma l_χ, and the characteristic radius of the DM particles distribution in the core of the star r_χ [e.g., [48,95]]. For most of the DM-nuclei scattering cross sections σ_χ ($\sigma_{SD,\chi}$ or $\sigma_{SI,\chi}$) considered here, in which $l_\chi \geq r_\chi$, the energy transport by DM is nonlocal. On the other hand, for large values of DM-nuclei scattering cross sections, in which $l_\chi \leq r_\chi$, the DM particles are in local thermal equilibrium with the baryons. This latter regime applies only to values of σ_χ which are not considered in this work ($\sigma_\chi \geq 10^{-33}$ cm^2). However, we follow the prescription described in Gould and Raffelt [96] that extends the formalism developed for the local thermal equilibrium to other regimes by the use of tabulated suppression factors. Moreover, once the characteristic radius of the DM core decreases with the mass of the DM particle, such as $r_\chi \propto m_\chi^{-1/2}$ [e.g., [95]]: stellar models computed for DM particles with different masses will produce the ^{8}B solar neutrino spectra with different shapes.

The main effect of this additional transport of energy is a decrease of temperature in the core of the Sun in relation to the standard solar model. This temperature variation is followed by an increase in the radial profiles of the density $\rho(r)$, and the mean molecular weight per electron $\mu_e(r)$. But as the increase of the density dominates over the increase of mean molecular weight per electron, and the electron density $n_e(r)$ is proportional to the ratio $\rho(r)/\mu_e(r)$, this leads to an overall increase of $n_e(r)$ at core of the star [e.g., [97]]. Moreover, as the MSW effect (i.e., the conversion of electron-neutrinos to other neutrino flavors) increases with $n_e(r)$, this process leads to a decrease of survival probability of electron-neutrino, as it will be discussed in Sec. V. Furthermore, as the proton-proton chain and carbon-nitrogen-oxygen cycle of nuclear reactions are much more sensitive to the local variations of temperature than density, for a nuclear reaction such as the ^{8}B β-decay process in the ^{8}B nuclear reaction rate, this temperature reduction necessarily leads to smaller ^{8}B solar neutrino flux.

IV. ^{8}B SOLAR ELECTRON-NEUTRINO SPECTRUM AND FLAVOR OSCILLATIONS

The ^{8}Bν_e spectrum emitted by the ^{8}B reaction in the Sun's core has been shown to be equivalent to several experimental determinations of the ^{8}Bν_e spectrum [e.g., [17,19]]. Bahcall and Holstein [98], Napolitano *et al.* [99] among others have shown that the ^{8}Bν_e neutrino spectrum emitted in the Sun's core is equal to the spectrum measured in the laboratory, as the surrounding solar plasma does not affect this type of nuclear reaction. Moreover, the ^{8}Bν_e experimental spectrum agrees remarkably well with the theoretical prediction for neutrinos with an energy below 12 MeV. In particular, the ^{8}Bν_e neutrino spectra deduced from four laboratory experiments [16,18–20,100] agrees within about 1% at high neutrino energies, whereas before they differed by 4% [18]. Figure 1 shows $\Psi^e_\odot(E_\nu)$, the ^{8}Bν_e spectrum emitted by the ^{8}B solar reaction in the Sun's core, with $\Psi^e_\oplus(E_\nu)$ and $\Psi^{\mu\tau}_\oplus(E_\nu)$, the two components of the ^{8}Bν_e neutrino spectrum measured on Earth. We note that the $\Psi^e_\odot(E_\nu)$ spectrum (cf. Fig. 1) is identical to the ^{8}Bν_e spectrum measured in the laboratory. Therefore, the only variation expected in the electron-neutrino spectrum measured by solar neutrino detectors, i.e., $\Psi^e_\oplus(E_\nu)$, is uniquely related to the neutrino flavor oscillations.

The fraction of electron-neutrinos that changes flavor depends on the parameters associated with vacuum and matter oscillations, and this latter process depends also on the local properties of the solar plasma [22]. This is the reason why $\Psi^e_\oplus(E_\nu)$ is significantly different from $\Psi^e_\odot(E_\nu)$. These quantities are related as follows:

$$\Psi^e_\oplus(E_\nu) = \langle P_{\nu_e}(E_\nu)\rangle \Psi^e_\odot(E_\nu) \tag{2}$$

where $\langle P_{\nu_e}(E_\nu)\rangle$ is the electron-neutrino survival probability of a neutrino of energy E_ν. $\langle P_{\nu_e}(E_\nu)\rangle$ reads

$$\langle P_{\nu_e}(E_\nu)\rangle = A^{-1}\int_0^{R_\odot} P_{\nu_e}(E_\nu, r)\Phi_\nu(r)4\pi\rho(r)r^2 dr, \tag{3}$$

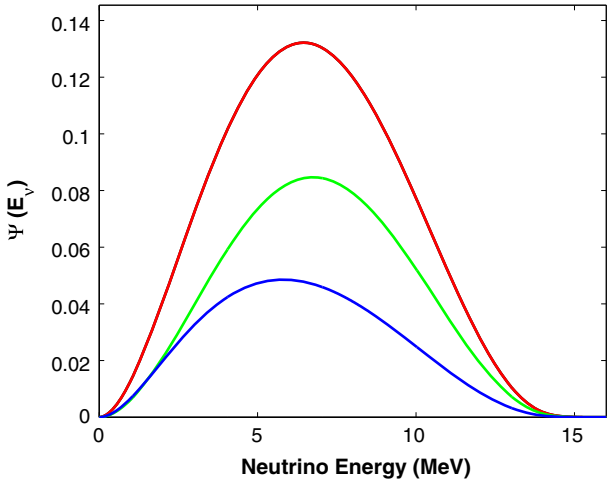

FIG. 1. The ^{8}Bν_e solar spectrum: $\Psi^e_\odot(E_\nu)$—electron-neutrino spectrum emitted in the Sun's core (red continuous curve); $\Psi^e_\oplus(E_\nu)$—electron-neutrino measured by neutrino detectors on Earth (blue continuous curve); $\Psi^{\mu\tau}_\oplus(E_\nu)$—nonelectron-neutrino spectrum (combine τ and μ neutrino spectrum) on Earth (green continuous curve). In the figure $\Psi^e_{...}(E_\nu)$ corresponds to the probability per MeV that a electron-neutrino is emitted with a energy E_ν. Notice that $\Psi^e_\odot(E_\nu) = \Psi^e_\oplus(E_\nu) + \Psi^{\mu\tau}_\oplus(E_\nu)$. This calculation used an up-to-date SSM (see text).

where $\Phi_\nu(r)$ is the ^{8}B electron-neutrino emission source. As usual, r is the solar radius, $\rho(r)$ is the density and A is a normalization constant. In the absence of matter-induced oscillations due to the Earth's atmosphere, $P_{\nu_e}(E_\nu, r)$ corresponds to the electron-neutrino survival probabilities on Earth during the day. It follows that $P_{\nu_e}(E_\nu, r) = \cos^4\theta_{13} P_{2\nu_e}(E_\nu, r) + \sin^4\theta_{13}$, where $P_{2\nu_e}(E_\nu, r)$ is the probability of a two-flavor neutrino oscillation model [e.g., [101–103]] and θ_{13} a neutrino mixing angle in vacuum. $P_{2\nu_e}(E_\nu, r)$ is given by

$$P_{2\nu_e}(E_\nu, r) = \frac{1}{2} + \frac{1}{2}\cos(2\theta_{21})\cos(2\theta_m), \tag{4}$$

where Δm_{12} is the mass difference between two flavors, θ_{21} is a flavor mixing angle in vacuum and θ_m is the matter mixing angle inside the Sun. θ_m reads

$$\sin(2\theta_m) = \frac{\sin(2\theta_{12})}{\sqrt{(V_m - \cos(2\theta_{12}))^2 + \sin^2(2\theta_{12})}}, \tag{5}$$

where $V_m(E_\nu, r) = 2\sqrt{2}G_f n_e(r) E_\nu \cos^2(\theta_{13})/\Delta m_{21}$, G_f is the Fermi constant and $n_e(r)$ is the electron density of the solar plasma. Equations (3)–(5) determine the probability of electron-neutrinos to be converted to other flavors when propagating in matter. This process can affect all solar neutrino sources, but it is more pronounced on the ^{8}Bν_e spectrum.

Figure 2 illustrates this specific point. In the figure it is shown the "theoretical" (dashed black curves) and the "observable" (colored curves) survival probability $\langle P_{\nu_e}(E_\nu)\rangle$ of electron-neutrinos[1] as a function of neutrino energy for the SSM. $\langle P_{\nu_e}(E_\nu)\rangle$ was computed for ^{8}Bν_e, as well as for other neutrino source reactions of the proton-proton chain and carbon-nitrogen-oxygen cycle. Although all neutrino's nuclear reaction sources occur in the Sun's core, the only ones that can be affected the structure changes due to accretion DM in the Sun's core are the ones that produce the neutrinos with the higher energy. This corresponds to the ^{8}B neutrinos (blue curve) and hep neutrinos (yellow curve), as shown in Fig. 2. Nevertheless, the former occur near the center of the Sun and are measured with much better precision that the hep neutrino spectrum. Therefore, the ^{8}Bν_e spectrum will be the most affected by the presence of the DM in the Sun's core.

The impact of DM on the $\langle P_{\nu_e}(E_\nu)\rangle$ or ^{8}Bν_e spectrum can be described as follows: In the Sun's interior, a neutrino

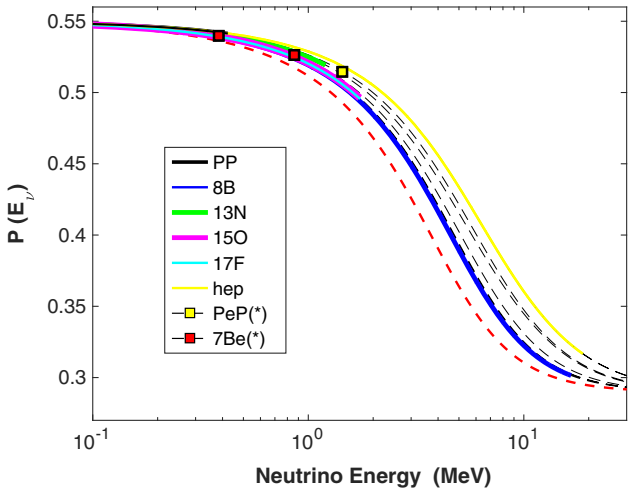

FIG. 2. The survival probability of electron-neutrinos as a function of the neutrino energy for a standard solar model. The colored parts of the curves indicates the energy range of neutrinos produced in the Sun's core for each nuclear reaction (as "measured" by solar neutrino experiments): ^{8}Bν_e (blue curve), ^{7}B$e\nu_e$ (two red-squares; emission lines), $pep\nu_e$ (yellow square, emission line), $hep\nu_e$ (yellow curve) $pp\nu_e$ (black curve), ^{13}Nν_e (green curve), ^{15}Oν_e (magenta curve), ^{17}Fν_e (cyan curve). The reference curve (red dashed curve) defines the survival probability of electron-neutrinos in the center of the Sun. The generic properties of such curves can be found in Lopes [22].

of energy E_ν can be converted to other flavors if $E_\nu \geq E_\nu^c(r)$. The quantity $E_\nu^c(r)$ defines the minimum (critical) energy that a neutrino must have to be strongly affected by flavor oscillations. $E\nu_c(r)$ is determined by the condition $V_m(E_\nu^c, r) = \cos(2\theta_{12})$ [from Eq. (5)], it follows that $E_\nu^c(r) = \Delta m_{21}/(2\sqrt{2}G_f)\cos(2\theta_{12})/\cos^2(\theta_{13})n_e^{-1}(r)$.

The survival probabilities of electron-neutrinos and $E_\nu^c(r)$ were computed by using the fundamental parameters of solar neutrino oscillations in the vacuum: Δm_{12} and θ_{12} as determined by the KamLAND experiment [102]. Although the contribution related to θ_{13} is very small, we take its contribution into account by choosing $\theta_{13} = 9$ deg, a value that is in agreement with current experimental measurements [104,105]. Figure 3 shows the critical value $E_\nu^c(r)$ for current SSM and other solar models: neutrinos experiment MSW flavor oscillations in regions of the Sun's core where the neutrino energy is such that $E_\nu \geq E_\nu^c$ (yellow region in Fig. 3), otherwise the effect is insignificant. The magnitude of flavor oscillations caused by matter depends on the local value of $n_e(r)$, namely the values of density and metallicity. These oscillations are only significant in the Sun's core and negligible in most of the radiative region and solar convection zone. The fraction of electron-neutrinos converted to other flavors depends also on the location of the neutrino source, as well as the local temperature as shown in Fig. 3.

[1]The "theoretical" $\langle P_{\nu_e}(E_\nu)\rangle$ although not directly related with the real solar spectrum unlike the "observable" $\langle P_{\nu_e}(E_\nu)\rangle$. This quantity illustrates well the effect that the energy dependence of neutrino matter oscillations have on the flux of electron-neutrinos.

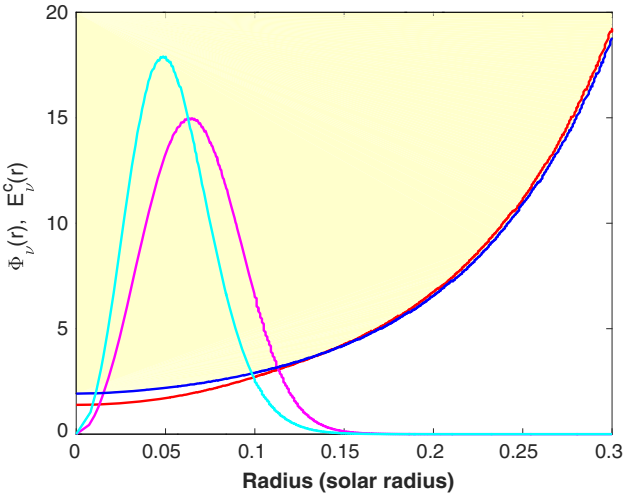

FIG. 3. Variation of the functions $\Phi_\nu(r)$ and $E\nu_c(r)$ (in MeV) with the fractional solar radius r. The cyan and blue curves correspond to $\Phi_\nu(r)$ and $E\nu_c(r)$ for the SSM, and the magenta and red curves are the equivalent ones for a DM solar model with the $m_\chi = 5$ GeV and $\sigma_{\chi,SI} = 10^{-36}$ cm^2. Both sets of curves have relatively similar shapes. Cyan and magenta curves: Φ_ν's is drawn as a function of r such that $\Phi_\nu(r) = F^{-1}df(r)/dr$ for which $f(r)$ is the ^{8}B neutrino flux in s^{-1} and F is the total neutrino flux for ^{8}B nuclear reaction rate. Blue and red curves: E^c_ν's represented as a function of r corresponds to the minimum neutrino energy E_ν that a neutrino must have in order to experience a resonance (see text). Accordingly, electron neutrinos such as $E_\nu \geq E^c_\nu(r)$ will experience matter flavor oscillations in the solar core, otherwise this effect is negligible.

V. DARK MATTER SIGNATURE ON ^{8}B NEUTRINO SPECTRUM

The presence of DM in the Sun's core changes its thermodynamic structure, modifying the temperature, density and chemical composition, as well as $n_e(r)$. Although the effect is relatively small, as neutrinos are very sensitive to the temperature of the Sun's core, minor variations in temperature produce variations in the ^{8}Bν_e spectrum. Consequently, the ^{8}B neutrino flux and ^{8}Bν_e spectrum are modified as a result of the variation of the magnitude and location of the ^{8}B neutrino source (cf. Fig. 3). In addition, the variation of $n_e(r)$ distorts the ^{8}Bν_e spectrum, due to an alteration of the survival probability of electron-neutrinos which determines the fraction of electron-neutrinos converted to other flavors. Different DM models have different critical neutrino energies E^c_ν, leading to distinct $\langle P_{\nu_e}(E_\nu)\rangle$ for ^{8}Bν_e and other neutrino sources (cf. Figs. 2–4). The combination of these different physical processes modifies the shape of $\Psi^e_\oplus(E_\nu)$, i.e., the ^{8}Bν_e spectrum measured in terrestrial detectors.

The ^{8}Bν_e spectrum is strongly dependent on the temperature, but also on the density and chemical composition. Actually, $\Psi^e_\oplus(E_\nu)$ the ^{8}Bν_e spectrum shape of the electron neutrino, is related to the variation of the density by three possibilities: the production rate of electron-neutrinos leading to the neutrino function $\Phi_\nu(r)$, the location of the maximum of $\Phi_\nu(r)$ and the survival probability of electron neutrinos [i.e., the conversion of electron-neutrinos to other flavors, Eq. (3)]:

The first two effects result from the fact that variations in total neutrino flux ϕ (or equally on the production rate of ^{8}B neutrinos) depend on the temperature T and density ρ as $\Delta\phi/\phi \approx \Delta\rho/\rho + \alpha\Delta T/T$ where $\alpha = 24.5$ is obtained from Chieze and Lopes [80]. Accordingly, a 10% variation on $\Delta\phi/\phi$ is either attributed to a variation in 10% of density, 0.4% in temperature, or a combination of both. Moreover, a similar variation on the molecular weight is also expected. Nevertheless, as mentioned by several authors [e.,g. [27,30,31]] as solar models are calibrated to have the observed solar radius and luminosity, the effective variation of ρ is smaller than the previous estimate, the mitigation coming from the temperature and chemical composition readjustment. The variation of $\Phi_\nu(r)$ leads to a slight change in the location of the maximum of $\Phi_\nu(r)$. This variation also influences the amount of electron-neutrinos converted to other flavors as described by equation (3).

Equally from Eq. (4), the variation of $\Delta P_e/P_e$ is proportional to the variation of electronic density $\Delta n_e/n_e$ (or density and molecular weight). The impact of DM on the electronic-neutrino survival probability function $\langle P_{\nu_e}(E_\nu)\rangle$ is shown in Fig. 4. As pointed out by previous authors [e.g., [22] and references therein] the effect on $\langle P_{\nu_e}(E_\nu)\rangle$ at first order is relatively small, as at

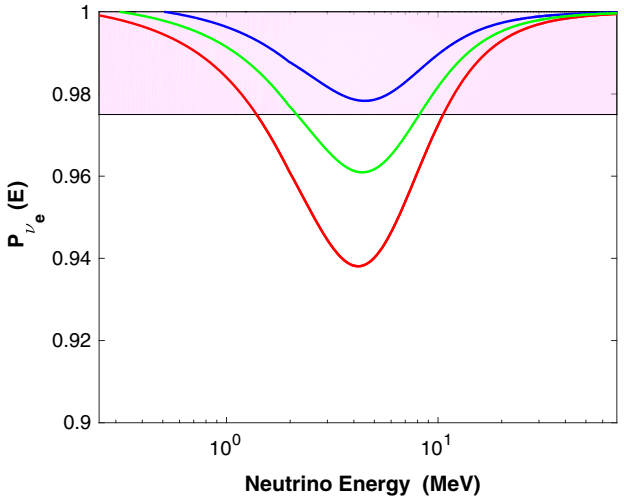

FIG. 4. The ratio of several ^{8}B survival probabilities of electron-neutrinos of DM solar models in relation to the standard solar model. The color curves correspond to an halo of DM particles with the following properties: $m_\chi = 4$ GeV and $\sigma_{\chi,SI} = 10^{-37}$ cm^2 (red curve); $m_\chi = 5$ GeV and $\sigma_{\chi,SI} = 10^{-35}$ cm^2 (green curve) and $m_\chi = 7$ GeV and $\sigma_{\chi,SI} = 10^{-35}$ cm^2 (blue curve). The pink area defines the experimental error bar of the LENA detector (see text).

low energies the neutrino oscillations are vacuum-related and therefore insensitive to the Sun's structure; for the higher energy neutrinos, the flavor oscillations are vacuum and density-related (see Fig. 3). The effect of the Sun's structure on $\langle P_{\nu_e}(E_\nu)\rangle$ is more pronounced for neutrinos with intermediate energies (from 0.1 to 1.0 MeV). As shown in Fig. 4, the variation of electronic density (density and molecular weight) with solar radius slightly changes the profile of $\langle P_{\nu_e}(E_\nu)\rangle$, leading to small changes in the shape of the ^{8}Bν_e spectrum (see Sec. III). Moreover, Fig. 4 shows the part of the ^{8}Bν_e spectrum that is more affected. This corresponds to neutrinos with an energy in the range: 1 to 10 MeV. This variation is more pronounced for light DM particles with the largest scattering cross sections. This effect reduces the ^{8}Bν_e electron survival probability curve by as much as 6% in relation to the standard case. It is important to observe that such effect on the electron survival probability will distort the electron-neutrino ^{8}B spectrum in the same neutrino energy range. Although this shape deformation is small, once future measurements of ^{8}B electron neutrinos will be able to possibly detect such types of effect, if observed it could provide a hint of the existence of dark matter. It is worth remembering that the shape of the ^{8}B neutrino spectrum is very well measured by current laboratory experiments (see introduction and references therein). For DM solar models discussed in this paper, the maximum effect observed in $\Psi^e_\oplus(E_\nu)$ uniquely related with $\langle P_{\nu_e}(E_\nu)\rangle$ is of the order of 6.5% and occurs near 6 MeV.

The identification by a future solar neutrino detector of a strong distortion in the shape of $\Psi^e_\oplus(E_\nu)$ compared to that predicted by the SSM, would constitute a strong hint for the presence of DM in the Sun's core. The magnitude of the distortion should give some indication about the amount of DM and the extension of the DM core. Figure 5 shows the difference for the ^{8}Bν_e spectrum for a DM solar model. This is due to the fact that ν_e neutrinos of different energy have a different sensitivity to the local distribution of electron density of the Sun's core, specifically, only the more energetic neutrinos are affected by matter flavor oscillations.

In this study we have explored how the presence of DM in the Sun's core changes the shape of solar neutrino spectra, for instance the ^{8}Bν_e neutrino spectrum. In many cases, the impact of DM in the Sun's core can be determined by variations on the total neutrino fluxes due to local temperature changes. Nonetheless, there is an important point to make: even for an identical percentage variation $\Psi^e_\oplus(E_\nu)$ and ϕ, there is a fundamental different between both quantities, as the former gives the location where the DM effect occurs (cf. Fig. 5). Indeed, the presence of DM in the solar core will distort $\Psi^e_\oplus(E_\nu)$ very likely around $E_\nu \sim 6$ MeV (although depending on the DM models, $\Psi^e_\oplus(E_\nu)$ could be quite singular) and not uniformly distributed, information that is not possible to obtain from ϕ. As ϕ is an integrated quantity $\Phi_\nu(r)$, this only give us very limited information about the radial distribution of the DM in the core.

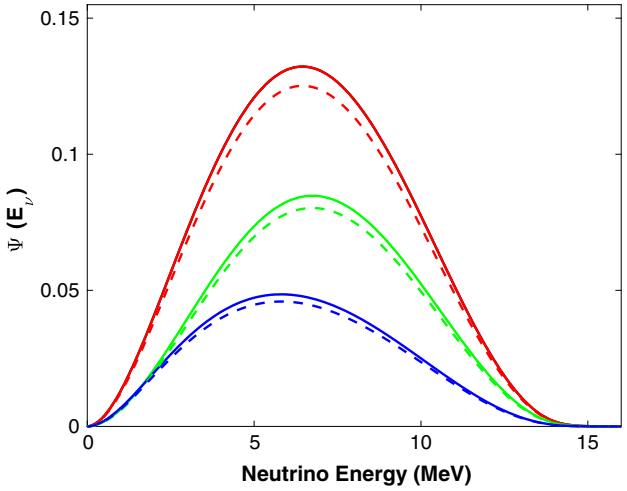

FIG. 5. The ^{8}Bν_e solar spectrum: the continuous corresponds to the SSM and the dashed curve to DM solar model with $m_\chi = 5$ GeV an $\sigma_{\chi,SI} = 10^{-36}$ cm^2. The color scheme is the same as the one used in Fig. 1.

Although this work is focused on studying the ^{8}Bν_e spectrum, our study is easily extended to other neutrino sources as shown in Fig. 2. However, there are currently no neutrino experiments planned to measure the spectrum of other solar neutrino sources in the near future.

VI. SUMMARY

In this paper, we have shown that a detailed measurement of the ^{8}Bν_e spectrum in the range from 1–15 MeV by future solar neutrino experiments will permit us to probe in great detail the core of the Sun (below $0.1R_\odot$) in a search for traces of DM. We have also shown that this type of DM diagnostic can be extended to other solar neutrino spectra, once the experimental data becomes available (cf. Fig. 2).

The SSM predicts that the ^{8}Bν_e earth spectrum, expected to be measured by solar neutrino detectors, is very different from the ^{8}Bν_e solar emitted spectrum, due to vacuum and matter oscillations which neutrinos experience when travelling to Earth. The presence of DM in the Sun's core will change the magnitude and shape of the ^{8}Bν_e spectrum for terrestrial observers in a very distinct manner. Since there are many astrophysics processes that are not yet included in the standard solar model, that could also affect the physics of Sun's core and the solar neutrino fluxes [e.g., [106]], the distortion of the ^{8}Bν spectrum is an additional important signature that could play a determinant role in disentangling the impact of DM from other possible physical processes. The next generation of solar neutrino detectors like JUNO [6] and LENA [3] should be able to achieve the required precision to test such solar DM models. This will

be achieved by simultaneously increasing the precision on the measurements of the solar neutrino spectrum (or the survival electron-neutrino probability) and also by increasing the energy resolution, without which it is not possible to precisely measure the shape distortion of the $^8B\nu_e$ spectrum. Moreover, it is expected that the LENA detector after only 5 years of measurements will be able to obtain a probability survival for electron-neutrino (or the equivalent $^8B\nu$ flux) with an experimental error smaller than 0.025 [107]. This precision is sufficient to put constrains in some solar DM models [108], since for some of them the survival electron-neutrino probability variation is of the order of 0.06 (cf. Figure 4). For instance, if we assume that such experimental accuracy is attained on LENA measurements, solar DM models with $m_\chi \leq 5$ GeV and $\sigma_{\chi,SI} \geq 10^{-35}$ cm^2 as the ones shown in Fig. 4 can be excluded using the putative LENA data set. This type of diagnostic could help to determine if light asymmetric DM is indeed present in the Sun's core, as this type of DM has been suggested as a nonstandard solution to resolve the solar abundance problem.

ACKNOWLEDGMENTS

The authors are grateful to the anonymous referee for the comments and suggestions which improved the overall quality this article. The author I. L. thanks the Fundação para a Ciência e Tecnologia (FCT), Portugal, for the financial support to the Center for Astrophysics and Gravitation (CENTRA/IST/ULisboa) through the Grant No. UID/FIS/00099/2013. The research of J. S. has been supported at IAP by the ERC Project No. 267117 (DARK) hosted by Université Pierre et Marie Curie—Paris 6 and at JHU by NSF Grant No. OIA-1124403. We are grateful to the authors of the DarkSUSY and CESAM codes for having made their codes publicly available.

[1] C. Giganti, S. Lavignac, and M. Zito, Prog. Part. Nucl. Phys. **98**, 1 (2018).
[2] W. C. Haxton, R. G. Hamish Robertson, and A. M. Serenelli, Annu. Rev. Astron. Astrophys. **51**, 21 (2013).
[3] M. Wurm, J. F. Beacom, L. B. Bezrukov *et al.*, Astropart. Phys. **35**, 685 (2012).
[4] A. de Gouvêa and K. J. Kelly, Nucl. Phys. **B908**, 318 (2016).
[5] J. F. Beacom, S. Chen, J. Cheng *et al.*, Chin. Phys. C **41**, 023002 (2017).
[6] F. An, G. An, Q. An *et al.*, J. Phys. G **43**, 030401 (2016).
[7] A. Bandyopadhyay, S. Choubey, R. Gandhi *et al.*, Rep. Prog. Phys. **72**, 106201 (2009).
[8] A. de Gouvea, K. Pitts, K. Scholberg *et al.*, arXiv: 1310.4340.
[9] A. B. Balantekin and H. Yüksel, Nucl. Phys. **B138**, 347 (2005).
[10] A. B. Balantekin, J. F. Beacom, and J. M. Fetter, Phys. Lett. B **427**, 317 (1998).
[11] J. H. Davis, Phys. Rev. Lett. **117**, 211101 (2016).
[12] I. Lopes, Astrophys. J. Lett. **777**, L7 (2013).
[13] I. Lopes, Phys. Rev. D **95**, 015023 (2017).
[14] A. Serenelli, C. Peña-Garay, and W. C. Haxton, Phys. Rev. D **87**, 043001 (2013).
[15] I. P. Lopes and J. Silk, Phys. Rev. Lett. **88**, 151303 (2002).
[16] O. S. Kirsebom, S. Hyldegaard, M. Alcorta *et al.*, Phys. Rev. C **83**, 065802 (2011).
[17] C. E. Ortiz, A. Garcia, R. A. Waltz, M. Bhattacharya, and A. K. Komives, Phys. Rev. Lett. **85**, 2909 (2000).
[18] T. Roger, J. Büscher, B. Bastin *et al.*, Phys. Rev. Lett. **108**, 162502 (2012).
[19] W. T. Winter, S. J. Freedman, K. E. Rehm, and J. P. Schiffer, Phys. Rev. C **73**, 025503 (2006).
[20] W. T. Winter, S. J. Freedman, K. E. Rehm *et al.*, Phys. Rev. Lett. **91**, 252501 (2003).
[21] J. N. Bahcall, Phys. Rev. D **44**, 1644 (1991).
[22] I. Lopes, Phys. Rev. D **88**, 045006 (2013).
[23] B. Pontecorvo, Sov. J. Exp. Theor. Phys. **6**, 429 (1958).
[24] L. Wolfenstein, Phys. Rev. D **17**, 2369 (1978).
[25] J. A. Guzik and K. Mussack, Astrophys. J. **713**, 1108 (2010).
[26] A. M. Serenelli, W. C. Haxton, and C. Peña-Garay, Astrophys. J. **743**, 24 (2011).
[27] A. Bottino, G. Fiorentini, N. Fornengo, B. Ricci, S. Scopel, and F. L. Villante, Phys. Rev. D **66**, 053005 (2002).
[28] S. Turck-Chieze, R. A. Garcia, I. Lopes, J. Ballot, S. Couvidat, S. Mathur, D. Salabert, and J. Silk, Astrophys. J. Lett. **746**, L12 (2012).
[29] J. Lopes and I. Lopes, Astrophys. J. **827**, 130 (2016).
[30] D. T. Cumberbatch, J. A. Guzik, J. Silk, L. S. Watson, and S. M. West, Phys. Rev. D **82**, 103503 (2010).
[31] M. T. Frandsen and S. Sarkar, Phys. Rev. Lett. **105**, 011301 (2010).
[32] F. Iocco, M. Taoso, F. Leclercq, and G. Meynet, Phys. Rev. Lett. **108**, 061301 (2012).
[33] I. Lopes and J. Silk, Astrophys. J. **757**, 130 (2012).
[34] M. Taoso, F. Iocco, G. Meynet, G. Bertone, and P. Eggenberger, Phys. Rev. D **82**, 083509 (2010).
[35] A. M. Serenelli, S. Basu, J. W. Ferguson, and M. Asplund, Astrophys. J. **705**, L123 (2009).
[36] I. Lopes, P. Panci, and J. Silk, Astrophys. J. **795**, 162 (2014).
[37] A. C. Vincent, A. Serenelli, and P. Scott, J. Cosmol. Astropart. Phys. 8 (2015) 040.
[38] J. Casanellas and I. Lopes, Astrophys. J. Lett. **765**, L21 (2013).

[39] A. Martins, I. Lopes, and J. Casanellas, Phys. Rev. D **95**, 023507 (2017).
[40] C. Kouvaris and P. Tinyakov, Phys. Rev. D **82**, 063531 (2010).
[41] C. Kouvaris and P. Tinyakov, Phys. Rev. D **83**, 083512 (2011).
[42] C. Kouvaris and P. Tinyakov, Phys. Rev. Lett. **107**, 091301 (2011).
[43] J. Kumar, in *Asymmetric Dark Matter*, American Institute of Physics Conference Series Vol. 1604 (AIP Conference, Deadwood, 2014), pp. 389–396.
[44] J. Casanellas and I. Lopes, Astrophys. J. Lett. **733**, L51 (2011).
[45] I. Lopes and J. Silk, Astrophys. J. **786**, 25 (2014).
[46] P. Scott, M. Fairbairn, and J. Edsjö, Mon. Not. R. Astron. Soc. **394**, 82 (2009).
[47] P. Scott, A. Venkatesan, E. Roebber, P. Gondolo, E. Pierpaoli, and G. Holder, Astrophys. J. **742**, 129 (2011).
[48] M. Taoso, G. Bertone, G. Meynet, and S. Ekström, Phys. Rev. D **78**, 123510 (2008).
[49] I. Lopes, K. Kadota, and J. Silk, Astrophys. J. Lett. **780**, L15 (2014).
[50] A. C. Vincent and P. Scott, J. Cosmol. Astropart. Phys. 4 (2014) 019.
[51] Planck Collaboration and 264 colleagues, Astron. Astrophys. **571**, A16 (2014).
[52] C. L. Bennett, D. Larson, J. L. Weiland *et al.*, Astrophys. J. Suppl. Ser. **208**, 20 (2013).
[53] K. Petraki and R. R. Volkas, Int. J. Mod. Phys. A **28**, 1330028 (2013).
[54] K. M. Zurek, Phys. Rep. **537**, 91 (2014).
[55] M. Carena, G. Nardini, M. Quirós, and C. E. M. Wagner, Nucl. Phys. **B812**, 243 (2009).
[56] J. B. Dent, S. Dutta, and R. J. Scherrer, Phys. Lett. B **687**, 275 (2010).
[57] B. Dutta and J. Kumar, Phys. Lett. B **699**, 364 (2011).
[58] P.-H. Gu, M. Lindner, U. Sarkar, and X. Zhang, Phys. Rev. D **83**, 055008 (2011).
[59] M. Drees, H. Iminniyaz, and M. Kakizaki, Phys. Rev. D **73**, 123502 (2006).
[60] H. Iminniyaz, M. Drees, and X. Chen, J. Cosmol. Astropart. Phys. 07 (2011) 003.
[61] K. Sigurdson, M. Doran, A. Kurylov, R. R. Caldwell, and M. Kamionkowski, Phys. Rev. D **70**, 083501 (2004).
[62] J. Baron *et al.*, Science **343**, 269 (2014).
[63] P. Panci, Nuovo Cimento Soc. Ital. Fis. **38C**, 28 (2015).
[64] R. Bernabei, P. Belli, F. Cappella *et al.*, Eur. Phys. J. C **56**, 333 (2008).
[65] R. Bernabei, P. Belli, F. Cappella *et al.*, Eur. Phys. J. C **67**, 39 (2010).
[66] C. E. Aalseth, P. S. Barbeau, N. S. Bowden *et al.*, Phys. Rev. Lett. **106**, 131301 (2011).
[67] C. E. Aalseth, P. S. Barbeau, J. Colaresi *et al.*, Phys. Rev. Lett. **107**, 141301 (2011).
[68] G. Angloher, M. Bauer, I. Bavykina *et al.*, Eur. Phys. J. C **72**, 1971 (2012).
[69] R. Agnese *et al.*, Phys. Rev. Lett. **111**, 251301 (2013).
[70] R. Agnese, Z. Ahmed, A. J. Anderson *et al.*, Phys. Rev. D **88**, 031104 (2013).
[71] E. Del Nobile, C. Kouvaris, and F. Sannino, Phys. Rev. D **84**, 027301 (2011).
[72] Z. Ahmed, D. S. Akerib, S. Arrenberg *et al.*, Phys. Rev. Lett. **106**, 131302 (2011).
[73] E. Aprile, K. Arisaka, F. Arneodo *et al.*, Phys. Rev. Lett. **107**, 131302 (2011).
[74] E. Aprile, M. Alfonsi, K. Arisaka *et al.*, Phys. Rev. Lett. **109**, 181301 (2012).
[75] D. S. Akerib *et al.*, Phys. Rev. Lett. **112**, 091303 (2014).
[76] M. Cirelli, E. Del Nobile, and P. Panci, J. Cosmol. Astropart. Phys. 10 (2013) 19.
[77] E. Del Nobile, C. Kouvaris, P. Panci, F. Sannino, and J. Virkajarvi, J. Cosmol. Astropart. Phys. 08 (2012) 010.
[78] R. Foot, Phys. Lett. B **728**, 45 (2014).
[79] N. Fornengo, P. Panci, and M. Regis, Phys. Rev. D **84**, 115002 (2011).
[80] S. Turck-Chieze and I. Lopes, Astrophys. J. **408**, 347 (1993).
[81] M. Asplund, N. Grevesse, A. J. Sauval, and P. Scott, Annu. Rev. Astron. Astrophys. **47**, 481 (2009); Eur. Phys. J. C **72**, 1971 (2009).
[82] P. Morel, Astron. Astrophys. **124**, 597 (1997).
[83] E. G. Adelberger, A. García, R. G. H. Robertson *et al.*, Rev. Mod. Phys. **83**, 195 (2011).
[84] S. Turck-Chièze, J. Phys. Conf. Ser. **665**, 012078 (2016).
[85] I. Lopes and J. Silk, Mon. Not. R. Astron. Soc. **435**, 2109 (2013).
[86] G. Jungman, M. Kamionkowski, and K. Griest, Phys. Rep. **267**, 195 (1996).
[87] G. Bertone, D. Hooper, and J. Silk, Phys. Rep. **405**, 279 (2005).
[88] A. Gould, Astrophys. J. **321**, 571 (1987).
[89] P. Gondolo, J. Edsjö, P. Ullio, L. Bergström, M. Schelke, and E. A. Baltz, J. Cosmol. Astropart. Phys. 07 (2004) 008.
[90] I. Lopes, J. Casanellas, and D. Eugénio, Phys. Rev. D **83**, 063521 (2011).
[91] G. Busoni, A. De Simone, and W.-C. Huang, J. Cosmol. Astropart. Phys. 07 (2013) 010.
[92] K. Griest and D. Seckel, Nucl. Phys. **B283**, 681 (1987).
[93] A. Gould, Astrophys. J. **356**, 302 (1990).
[94] E. I. Gates, G. Gyuk, and M. S. Turner, Astrophys. J. Lett. **449**, L123 (1995).
[95] I. P. Lopes, J. Silk, and S. H. Hansen, Mon. Not. R. Astron. Soc. **331**, 361 (2002).
[96] A. Gould and G. Raffelt, Astrophys. J. **352**, 654 (1990).
[97] D. D. Clayton, *Principles of stellar evolution and nucleosynthesis* (University of Chicago Press, Chicago, 1983).
[98] J. N. Bahcall and B. R. Holstein, Phys. Rev. C **33**, 2121 (1986).
[99] J. Napolitano, S. J. Freedman, and J. Camp, Phys. Rev. C **36**, 298 (1987).
[100] M. Bhattacharya, E. G. Adelberger, and H. E. Swanson, Phys. Rev. C **73**, 055802 (2006).
[101] S. Bilenky, *Introduction to the Physics of Massive and Mixed Neutrinos*, Lecture Notes in Physics (Springer Verlag, Berlin, 2010), p. 817.
[102] A. Gando, Y. Gando, K. Ichimura *et al.*, Phys. Rev. D **83**, 052002 (2011).
[103] L. Landau and L. Rosenkewitsch, Z. Phys. **78**, 847 (1932).

[104] G. L. Fogli, E. Lisi, A. Marrone, D. Montanino, A. Palazzo, and A. M. Rotunno *et al.*, Phys. Rev. D **86**, 013012 (2012).
[105] D. V. Forero, M. Tórtola, and J. W. F. Valle, Phys. Rev. D **86**, 073012 (2012).
[106] I. Lopes, Solar models and neutrinos, in *Proceedings of the XXVIII International Conference on Neutrino Physics and Astrophysics, 2018, Heidelberg, Germany*, https://doi.org/10.5281/zenodo.1286864.
[107] R. Möllenberg, F. von Feilitzsch, and D. Hellgartner, L. Oberauer, M. Tippmann, J. Winter, M. Wurm, and V. Zimmer, Phys. Lett. B **737**, 251 (2014).
[108] I. Lopes and J. Silk, Science **330**, 462 (2010).